A priori assessment of a simple approach to evaluating burning rate in large eddy simulations of premixed turbulent combustion

RESEARCH ARTICLE | NOVEMBER 14 2024

A priori assessment of a simple approach to evaluating burning rate in large eddy simulations of premixed turbulent combustion

Andrei N. Lipatnikov

Physics of Fluids 36, 115152 (2024)
https://doi.org/10.1063/5.0239276

Physics of Fluids ARTICLE pubs.aip.org/aip/pof

A priori assessment of a simple approach to evaluating burning rate in large eddy simulations of premixed turbulent combustion

Cite as: Phys. Fluids **36**, 115152 (2024); doi: 10.1063/5.0239276
Submitted: 18 September 2024 · Accepted: 27 October 2024 ·
Published Online: 14 November 2024

View Online Export Citation CrossMark

Andrei N. Lipatnikov[a)]

AFFILIATIONS

Department of Mechanics and Maritime Sciences, Chalmers University of Technology, Gothenburg SE-412 96, Sweden

[a)]Author to whom correspondence should be addressed: lipatn@chalmers.se

ABSTRACT

This paper aims at assessing a hypothesis that resolution required to evaluate fuel consumption and heat release rates by directly (i.e., without a subgrid model of unresolved influence of small-scale turbulent eddies on the local flame) processing filtered fields of density, temperature, and species mass fractions should be significantly finer than resolution required to directly compute flame surface density by processing the same filtered fields. For this purpose, box filters of various widths Δ are applied to three-dimensional direct numerical simulation data obtained earlier from a statistically one-dimensional and planar, moderately lean H_2/air complex-chemistry flame propagating in a box under conditions of sufficiently intense small-scale turbulence (Karlovitz number is larger than unity, and a ratio of laminar flame thickness δ_L to Kolmogorov length scale is about 20). Results confirm this hypothesis and show that the mean flame surface density and area can be predicted with acceptable accuracy by processing filtered combustion progress variable fields computed using a sufficiently wide filter, e.g., $\Delta/\delta_L = 4/3$. Such an approach does not require a model of the influence of subgrid turbulent eddies on flame surface density provided that Δ and δ_L are of the same order of magnitude. Good performance of this approach is attributed to inability of small-scale (when compared to δ_L) turbulent eddies to substantially change the local flame structure, which, nevertheless, is significantly perturbed by larger turbulent eddies that strain the local flame.

 https://doi.org/10.1063/5.0239276

I. INTRODUCTION

The problem of evaluation of mean reaction rates in turbulent flames stems from a highly non-linear dependence of rates of many important reactions on temperature and has been challenging the combustion community over decades. Earlier, a number of models were developed to compute mean reaction rates within the framework of the Reynolds-averaged Navier–Stokes (RANS) approach, as reviewed elsewhere.[1,2] Today, the focus of computational fluid dynamics (CFD) studies of turbulent burning is shifted to large eddy simulations (LES),[3–6] which deal with quantities filtered over sufficiently small volumes, thus, allowing researchers to explore flame dynamics by directly resolving local processes in a wide range of turbulence spectrum. However, scales associated with the influence of the smallest turbulent eddies on the local flame are rarely resolved, and such subgrid effects still require modeling. For this purpose, both LES counterparts of RANS models and LES-specific models were developed. The former group involves, e.g., flame surface density (FSD) or flame wrinkling models,[7–10] scalar dissipation rate models,[9–11] presumed probability density function (PDF) models,[12,13] transported PDF approach,[14,15] conditional moment closure,[16–18] multiple mapping conditioning[19–21] methods, etc. Thickened flame models[22,23] and dynamic methods[24–26] are well-known members of the latter group.

Rapid progress in computer hardware and software has continuously been extending the range of scales resolvable in LES of turbulent burning, thus, enabling a resolution of several computational cells per laminar flame thickness in simulations of laboratory measurements. Accordingly, there is a growing body of LES studies[27–38] that do not invoke any model of the influence of small-scale turbulence on a flame (henceforth, "a combustion model" for brevity), but directly evaluate filtered reaction rates using the locally filtered values of density, temperature, and species mass fractions. In other words, equations that are hold for local fields are directly applied to filtered fields, thus, neglecting non-linear effects addressed by various combustion models.[7–21] For such a "direct" or no-combustion-model (noCM) approach to perform well, numerical resolution is expected to be significantly finer when compared to conventional LES studies that invoke a model of the influence of unresolved scales on filtered quantities. Indeed, recent *a posteriori* studies supported this noCM approach, provided that a ratio of filter width Δ to laminar flame thickness δ_L is sufficiently small, e.g., 0.25,[37] 0.20,[29] 0.125,[36] or even 0.05.[38] On the contrary, LES results[34] computed using different combustion models show that, if $\Delta \cong \delta_L$, the simplest noCM approach performs substantially worse than other models assessed in the cited paper. Results of *a priori* studies,[39–42] obtained by filtering direct numerical simulation (DNS) data, also show that numerical resolution required by this approach is significantly finer than laminar flames thickness, e.g., $\Delta = 0.2\delta_L$.[41] However, so fine resolution does not seem to be feasible in applied CFD research into turbulent combustion under elevated pressures and elevated temperatures in engines, where the thickness δ_L is very small.[42]

Nevertheless, there seems to be another way to run LES of turbulent burning without any combustion model. First, starting from the pioneering work by Damköhler,[43] an increase in burning velocity U_t by turbulence is often attributed mainly to an increase δA in flame surface area stretched by turbulent eddies. Recent DNS studies[44–47] do show that $U_t \cong S_L\delta A$ even in moderately lean H_2/air turbulent flames,[45] see also Fig. 1 in Sec. II, or in equidiffusive highly turbulent flames,[46] where local flame speed can differ significantly from the laminar flame speed S_L and be even negative.[45,46] In very lean hydrogen/air turbulent flames, U_t can be significantly larger than $S_L\delta A$ due to differential diffusion effects[46] reviewed elsewhere.[48] Since there is no widely accepted model for predicting such a significant increase in U_t/S_L due to these effects, they are beyond the scope of this work, whose focus is solely placed on comparing different approaches to LES of premixed flames characterized by $U_t \cong S_L\delta A$.

Second, various experimental and numerical data indicate that the flame surface area is weakly affected by small-scale (when compared to δ_L) turbulent eddies. For instance, measurements and computations of interaction of a laminar flame with a single vortex or a vortex pair show that too small vortices decay rapidly and do not substantially perturb the flame, see review articles[49,50] and recent papers.[51,52] Moreover, small-scale turbulent eddies may weakly affect a premixed flame, because residence time of the eddies within the flame is significantly reduced due to combustion-induced acceleration of the local flow in the flame-normal direction.[53,54] Accordingly, measurements of fractal characteristics of flame surfaces in turbulent flows, reviewed elsewhere,[55] show that inner cutoff scale of the surface wrinkles is significantly (by a factor of three or more) larger than δ_L. Recent DNS data[56–58] also indicate weak influence of small-scale turbulent eddies on a flame surface. For instance, relative contribution of eddies smaller than $2\,\delta_L$ to the total tangential strain rate of flame surface was reported to be as low as 0.1.[57,58]

Therefore, exploring the following hypothesis appears to be of interest: If LES aims at computing filtered flame surface area δA, rather than filtered reaction rates, then, the use of a moderately fine mesh (e.g., $\Delta \cong \delta_L$) could allow researchers to directly (i.e., without a flame surface density or flame wrinkling model[7–10]) evaluate the area by processing filtered scalar fields and, subsequently, find turbulent burning velocity $U_t \cong S_L\delta A$. The present work aims at (i) assessing this simple hypothesis and (ii) comparing resolution requirements associated with direct evaluation of filtered surface area and filtered reaction rates.

For these purposes, the DNS database created by Dave *et al.*[59] and Dave and Chaudhuri[60] and analyzed also by the present author[42,54,61–65] will be used. The DNS attributes and applied diagnostic tools are briefly described in Sec. II. Results are reported and discussed in Sec. III, followed by conclusions.

II. DNS ATTRIBUTES AND DIAGNOSTIC METHODS

Since the DNS attributes are reported elsewhere,[42,54,59–65] only their summary is given below.

A statistically planar and one-dimensional, lean hydrogen-air turbulent flame propagating in a cuboid ($19.18 \times 4.8 \times 4.8$ mm^3) was studied by adopting the Pencil code[66] to numerically solve unsteady and three-dimensional continuity, compressible Navier–Stokes, species and energy transport equations supplemented with the mixture-averaged molecular transport model (i.e., differences in molecular transfer coefficients of various species were taken into account in the simulations by Dave *et al.*[59] and Dave and Chaudhuri[60]) and a detailed chemical mechanism (9 species and 21 reactions) by Li *et al.*[67] The cuboid was meshed with a uniform grid of $960 \times 240 \times 240$ cells. At the transverse sides, boundary conditions were periodic. At the inlet and outlet, Navier–Stokes characteristic boundary conditions[68] were set.

To pre-generate homogeneous isotropic turbulence in another cube with the periodic boundary conditions, large-scale forcing was adopted.[59] The turbulence was allowed to evolve until a statistically stationary state was reached. At this final stage,[59] the rms velocity $u' = 6.7$ m/s; an integral length scale $L = 3.1$ mm; the integral timescale $\tau_t = L/u' = 0.46$ ms; turbulent Reynolds number $Re_t = u'L/\nu = 950$; Kolmogorov timescale $\tau_\eta = \left(\nu/\langle\varepsilon\rangle\right)^{1/2} = 0.015$ ms; and Kolmogorov length scale $\eta = \left(\nu^3/\langle\varepsilon\rangle\right)^{1/4} = 0.018$ mm. Here, $\langle\varepsilon\rangle = \langle 2\nu S_{ij}S_{ij}\rangle$ is the turbulence dissipation rate averaged over the cube; ν is the gas kinematic viscosity; $S_{ij} = \left(\partial u_i/\partial x_j + \partial u_j/\partial x_i\right)/2$ is the rate-of-strain tensor; and the summation convention applies to repeated indexes.

At $t = 0$, a pre-computed planar laminar flame (the equivalence ratio $\Phi = 0.81$, pressure $P = 1$ bar, and unburned gas temperature $T_u = 310$ K) was embedded into the cuboid at $x = x_0$. The laminar flame speed S_L, thickness $\delta_L^T = (T_b - T_u)/\max|\nabla T|$, and timescale $\tau_f = \delta_L^T/S_L$ are equal to 1.84 m/s, 0.36 mm, and 0.20 ms, respectively. Here, subscripts u and b designate unburned and burned gases, respectively. Subsequently, the flame was wrinkled and stretched by the pre-generated turbulence, which was continuously injected into the computational domain through its left boundary $x = 0$ and decayed along the x-direction.

The Karlovitz number $Ka = \tau_f/\tau_\eta$ and the Damköhler number $Da = \tau_t/\tau_f$, evaluated using characteristics of the pre-generated turbulence, are equal to 13 and 2.35, respectively. Due to decay of the injected statistically stationary turbulence with distance x from the inlet, the turbulence characteristics averaged over the cuboid cross section nearest to a plane where $\bar{c}_T(x) = 0.01$ (leading edge of the mean flame brush) are different:[54] $u' = 3.3$ m/s; Taylor length scale $\lambda = \sqrt{10\nu_u\bar{k}/\bar{\varepsilon}} = 0.25$ mm or $0.69\delta_L^T$; $\eta = 0.018$ mm or $0.05\delta_L^T$; $\tau_\eta = 0.087$ ms; $Re_\lambda = u'\lambda/\nu_u = 55$; and $Ka = 2.3$ is much less than $(\delta_L/\eta)^2 \cong 400$, because $S_L\delta_L/\nu_u \gg 1$ in moderately lean hydrogen-air mixtures.[69] Here, $k = u_j'u_j'/2$ is turbulent kinetic energy; $u_j' = u_j - \bar{u}_j$ designates j-th component of fluctuating velocity vector; $c_T = (T - T_u)/(T_b - T_u)$ is a temperature-based combustion progress variable; and overbars refer to time- and transverse-averaged quantities sampled at 55 instants from 1.29 to 1.57 ms.

Based on the reported values of Ka and, especially, $(\delta_L/\eta)^2$, the studied flame might be associated with a highly turbulent regime of premixed burning, called "stirred reactors", "thickened flames", or "broken reaction zones" in combustion regime diagrams invented by Williams,[70] Borghi,[71] and Peters,[72] respectively, by considering single-step-chemistry equidiffusive flames characterized by $Ka = (\delta_L/\eta)^2$. However, previous analyses[54,61,62,64] of these complex-chemistry DNS data[59,60] showed that local flames statistically retained the structure of the unperturbed laminar flame. Therefore, the studied case is associated with the flamelet combustion regime,[70–72] in line with numerous other recent experimental and DNS data reviewed elsewhere,[73–75] which indicate that turbulent combustion can occur in the flamelet regime at Karlovitz numbers significantly larger than unity. This phenomenon could be attributed, e.g., to the weak influence of the smallest turbulent eddies on the local flame structure, as discussed in Sec. I.

The focus of the present analysis is placed on the influence of the width Δ of a box filter applied to the DNS data on (i) generalized flame surface density $|\nabla \widehat{c_F}|$ or $|\nabla \widehat{c_T}|$ and (ii) fuel consumption rate $\widehat{\dot\omega_F} \equiv \dot\omega_F(\widehat\rho, \widehat T, \widehat{Y_k})$ or heat release rate $\widehat{\dot\omega_T} \equiv \dot\omega_T(\widehat\rho, \widehat T, \widehat{Y_k})$ evaluated using filtered density $\widehat\rho(\mathbf{x}, t)$, temperature $\widehat T(\mathbf{x}, t)$, and species mass fraction $\widehat{Y_k}(\mathbf{x}, t)$. Here, $c_F = 1 - Y_F/Y_{F,u}$ is a fuel-based combustion progress variable, $\widehat q(\mathbf{x}, t)$ designates filtered value of the quantity $q(\mathbf{x}, t)$, and the filter width Δ is varied from $0.11\delta_L$ to $4.44\delta_L$.

Reported for these purposes are spatial variations of time- and transverse-averaged values $\overline{\widehat q}(\bar c_F)$ of the aforementioned filtered quantities within the mean flame brush, with the x-dependence of $\overline{\widehat q}(x)$ being converted to its $\bar c_F$-dependence using the monotonous profile $\bar c_F(x)$ of time- and transverse-averaged fuel-based combustion progress variable. Moreover, the following integrals:

$$\delta A_T(t) = \frac{1}{A_0}\iiint |\nabla \widehat{c_T}|(\mathbf{x}, t)d\mathbf{x}, \quad (1)$$

$$\delta A_F(t) = \frac{1}{A_0}\iiint |\nabla \widehat{c_F}|(\mathbf{x}, t)d\mathbf{x}, \quad (2)$$

which characterize filtered flame surface areas for various Δ, will be compared with normalized turbulent burning velocities evaluated by integrating the raw DNS data over the computational domain, i.e.,

$$\frac{U_t^T(t)}{S_L} = \frac{1}{\rho_u S_L (T_b - T_u) A_0}\iiint \dot\omega_T(\mathbf{x}, t)d\mathbf{x}, \quad (3)$$

$$\frac{U_t^F(t)}{S_L} = -\frac{W_F}{\rho_u S_L X_{F,u} A_0}\iiint \dot\omega_F(\mathbf{x}, t)d\mathbf{x}. \quad (4)$$

Here, A_0 is the cuboid cross section area; W_F is fuel molecular weight; the rates $\dot\omega_T(\mathbf{x}, t)$ and $\dot\omega_F(\mathbf{x}, t)$ are measured in gK/(cm^{3}s) and mole/(cm^{3}s), respectively; $X_{F,u}$ is fuel mole fraction in unburned lean mixture; and subscript and superscript F or T refer to fuel-based (fuel concentration and consumption rate) or temperature-based (temperature and heat release rate) framework. When discussing trends observed in both frameworks, subscripts or superscripts F and H will be omitted in the following.

It is worth noting that, strictly speaking, flame surface area, i.e., the area of an iso-scalar surface $c(\mathbf{x}, t) = c^*$, associated with the flame front, should be evaluated by integrating $|\nabla c|\delta(c–c^*)$ over the flame brush volume.[1,76] Here, $\delta(c–c^*)$ is the Dirac delta function. Nevertheless, the generalized flame surface density $|\nabla c|$ is widely used in the literature[1] due to its simplicity. For the present goal, i.e., assessment of the simplest approach to LES of premixed turbulent flame, the use of the simplest characteristic of flame surface density, i.e., $|\nabla c|$, appears to be adequate, especially as this approach yields good results, see Fig. 1 and figures presented in the next section. From the fundamental perspective, since $\rho_u S_L|\nabla c| = \nabla\cdot(\rho D \nabla c) + \dot\omega$ everywhere within an unperturbed laminar flame, integration of $\rho_u S_L|\nabla c|$ and $\rho_u S_L|\nabla c|\delta(c–c^*)$ over flame brush volume should yield close values of burning velocity in the flamelet combustion regime, i.e., when local flames statistically retain the structure of the unperturbed laminar flame. Here, D is molecular diffusivity of c.

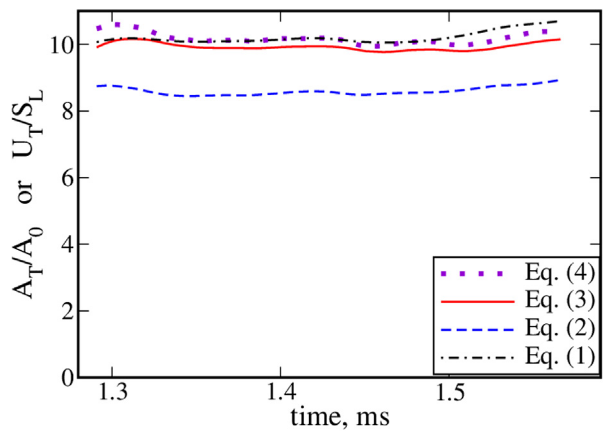

FIG. 1. Evolution of normalized turbulent burning velocities U_t/S_L(violet dotted and red solid lines) and generalized flame surface area $A_0^{-1}\iiint|\nabla c|d\mathbf{x}$ (blue dashed and black dotted-dashed lines) sampled from the DNS data within fuel (violet dotted and blue dashed lines) or temperature (red solid and black dotted-dashed lines) framework.

The direct comparison of $\delta A(t)$ and $U_t(t)/S_L$ is justified in Fig. 1, which shows that $U_t(t)/S_L$ is close to the area increase $\delta A(t)$ sampled directly from the DNS data, i.e., calculated by substituting $|\nabla \widehat c|(\mathbf{x}, t)$ with $|\nabla c|(\mathbf{x}, t)$ in Eq. (1) or (2). This trend is well pronounced within the temperature framework, i.e., when $U_T^T(t)/S_L$ is compared with $\delta A_T(t)$. Differences in $U_T^F(t)/S_L$ and $\delta A_F(t)$ are larger and can reach 15%. These differences could be attributed to differential diffusion effects, which are expected to increase a ratio of $U_t^F/(S_L\delta A_F)$ in lean H_2-air mixtures.[48] However, under conditions of the present study, the effect magnitude is quite moderate, i.e., less than 1.15. For comparison, values of $U_t^F/(S_L\delta A_F)$ as large as 2.4 and 5.8 have been obtained in a recent DNS study[77] of H_2-air flames characterized by $\Phi = 0.5$ and $\Phi = 0.35$, respectively.

So low magnitude of differential diffusion effects at $\Phi = 0.81$ is consistent with contemporary knowledge. Indeed, first, a complex-chemistry DNS study[78] of two-dimensional laminar flames indicates that differential diffusion effects contribute weakly to growth rate of flame surface perturbations when compared to hydrodynamic instability at $\Phi = 0.75$, i.e., in other words, these effects are weak at $\Phi = 0.75$. Second, DNS data obtained by several research groups[45,77,79,80] from different hydrogen-air turbulent flames characterized by $\Phi = 0.7$ indicate moderate differences between $U_t^F/(S_L\delta A_F)$ and unity, i.e., $1 < U_t^F/(S_L\delta A_F) < 1.5$. Since this difference is decreased[77,81] with increasing Φ, the close-to-unity value of $U_t^F/(S_L\delta A_F) \approx 1.15$ is not surprising at $\Phi = 0.81$.

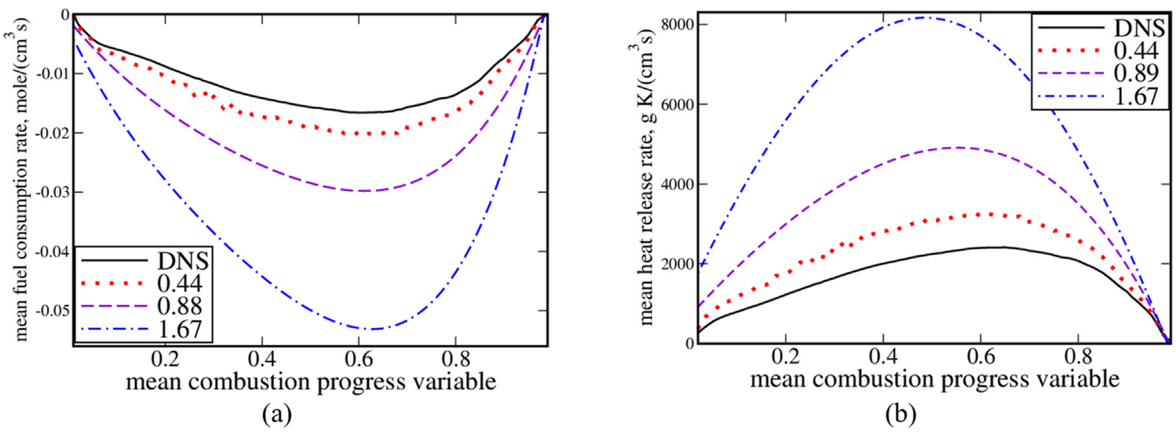

FIG. 2. Time- and transverse-averaged (a) fuel consumption and (b) heat release rates. Color broken lines show the rates $\overline{\dot{\omega}_F\left(\widehat{\rho},\widehat{T},\widehat{Y}_k\right)}$ or $\overline{\dot{\omega}_T\left(\widehat{\rho},\widehat{T},\widehat{Y}_k\right)}$ evaluated using quantities filtered over various boxes whose normalized widths Δ/δ_L are reported in legends. Black solid lines show the rates $\overline{\dot{\omega}_F(\rho,T,Y_k)}$ or $\overline{\dot{\omega}_T(\rho,T,Y_k)}$ sampled directly from the DNS data.

Finally, it is also worth noting that differences in the influence of differential diffusion on the fuel-based $U_t^F/(S_L\delta A_F)\approx 1.15$ and the temperature-based $U_t^T/(S_L\delta A_T)\approx 1$, observed in Fig. 1, are not surprising either. Indeed, several DNS studies[82–86] reported that differential diffusion effects caused substantially different variations in local fuel consumption and heat release rates. For instance, the highest local fuel consumption rates were documented in positively curved reaction zones and were attributed to high diffusivity of H_2, whereas the highest local heat release rates were documented[83–86] in negatively curved reaction zones and were attributed to high diffusivity of H.

III. RESULTS AND DISCUSSION

Figure 2 reports spatial variations of time- and transverse-averaged (a) fuel consumption and (b) heat release rates. It shows that the magnitude of the mean rate $\overline{\dot{\omega}_F}$ or $\overline{\dot{\omega}_T}$, sampled directly from the DNS data (see curves plotted in black solid lines), is overestimated if the counterpart filtered rate $\widehat{\dot{\omega}}_F$ or $\widehat{\dot{\omega}}_T$ is calculated using filtered density, temperature, and species mass fractions, i.e., $\widehat{\dot{\omega}}_F=\dot{\omega}_F\left(\widehat{\rho},\widehat{T},\widehat{Y}_k\right)$ or $\widehat{\dot{\omega}}_T=\dot{\omega}_T\left(\widehat{\rho},\widehat{T},\widehat{Y}_k\right)$, respectively, followed by time- and transverse-averaging (see curves plotted in color broken lines). Note that the rates $\overline{\dot{\omega}_F(\widehat{\rho,T,Y_k})}$ and $\overline{\dot{\omega}_T(\widehat{\rho,T,Y_k})}$ calculated by filtering the fields $\dot{\omega}_F(\mathbf{x},t)$ and $\dot{\omega}_T(\mathbf{x},t)$, respectively, followed by time- and transverse-averaging, are close[42] to the counterpart time- and transverse-averaged rates $\overline{\dot{\omega}_F}$ and $\overline{\dot{\omega}_T}$, respectively, sampled from the DNS data (not shown for brevity). In Fig. 2, differences between $\overline{\dot{\omega}_F}$ or $\overline{\dot{\omega}_T}$ (black solid lines) and the noCM rate $\overline{\widehat{\dot{\omega}}_F}$ or $\overline{\widehat{\dot{\omega}}_T}$, respectively, are substantial even if the filter width Δ is as low as $0.44\delta_L^T$ (red dotted lines), with the differences being about 100% if $\Delta=0.89\delta_L^T$ (violet dashed lines) or even much larger if $\Delta=1.67\delta_L^T$ (blue dotted-dashed lines).

On the contrary, Fig. 3 shows that differences in $\overline{|\nabla c_F|}$ or $\overline{|\nabla c_T|}$ sampled directly from the DNS data (black dots) and $\overline{|\nabla \widehat{c}_F|}$ or $\overline{|\nabla \widehat{c}_T|}$, respectively, are very small if $\Delta=0.33\delta_L^T$ (red solid lines) or $\Delta=0.67\delta_L^T$ (blue dashed lines) and remain moderate even if the filter

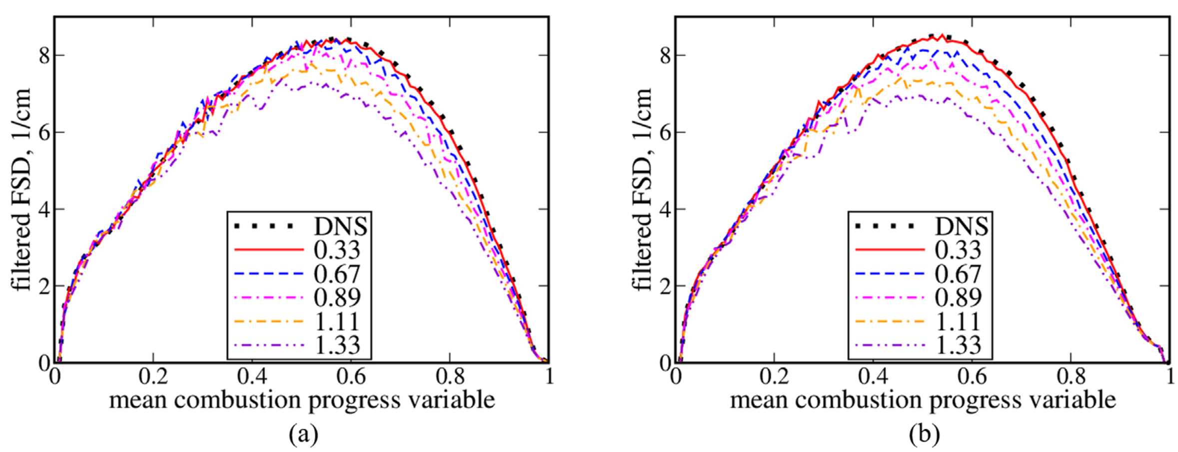

FIG. 3. Time- and transverse-averaged (a) fuel-based and (b) temperature-based generalized flame surface densities $\overline{|\nabla\widehat{c}|}$ filtered (lines) using various boxes whose normalized widths Δ/δ_L^T are reported in legends. Black dots show $\overline{|\nabla c|}$ sampled directly from the raw DNS data.

width Δ is larger than δ_L^T (orange dotted-double-dashed and violet double-dotted-dashed lines).

Thus, comparison of Figs. 2 and 3 implies that LES resolution requirements are significantly softer when invoking an FSD-based model of premixed turbulent burning when compared to direct calculation of filtered reaction rates using filtered density, temperature, and species mass fractions. For instance, Fig. 4(a) shows that comparable relative errors $\max\left\{\left|\overline{q}(\overline{c}) - \overline{\widehat{q}}(\overline{c})\right|\right\}/\max\left\{\left|\overline{q}(\overline{c})\right|\right\}$ are obtained for $q = \dot{\omega}_F$ or $\dot{\omega}_T$ using $\Delta = 0.44\delta_L^T$ and for $q = |\nabla c_F|$ or $|\nabla c_T|$ using $\Delta = 1.33\delta_L^T$, see horizontal and vertical straight dotted-dashed lines. Here, $\overline{q}(\overline{c})$ and $\overline{\widehat{q}}(\overline{c})$ designate time- and transverse-averaged DNS and filtered fields, $q(\mathbf{x},t)$ and $\widehat{q}(\mathbf{x},t)$, respectively. It is worth stressing that an increase in resolution by a factor of three (from $\Delta = 0.44\delta_L^T$ to $\Delta = 1.33\delta_L^T$) reduces numerical costs of unsteady three-dimensional simulations by a factor or 3^4=81. Moreover, a comparison of the influence of Δ on different quantities ($\overline{\dot{\omega}_F}$ or $\overline{\dot{\omega}_T}$ and $\overline{|\nabla c_F|}$ or $\overline{|\nabla c_T|}$, respectively) is justified in Fig. 1, which shows that differences between turbulent burning velocity obtained by integrating (i) $\dot{\omega}_F(\mathbf{x},t)$ or $\dot{\omega}_T(\mathbf{x},t)$ and (ii) $S_L|\nabla c_F(\mathbf{x},t)|$ or $S_L|\nabla c_T(\mathbf{x},t)|$, respectively, where S_L is constant, are quite moderate, i.e., about 15% in the fuel-based framework and much smaller in the temperature-based framework.

The highlighted difference in resolution requirements is also observed in Fig. 4(b), which reports ratios of (i) time-averaged turbulent burning velocity $\overline{U_t}$ (orange dotted-dashed or black dotted-double-dashed line) or (ii) time-averaged flame-surface-density integral $\overline{\delta A}$ (red solid or blue dashed line), obtained from filtered fields, to the counterpart quantity, $\overline{U_t}$ or $\overline{\delta A}$, respectively, sampled directly from the DNS data. The $\overline{U_t}$-ratios increase rapidly with Δ/δ_L^T and are about three at $\Delta/\delta_L^T = 1.67$. On the contrary, the $\overline{\delta A}$-ratios decrease slowly with Δ/δ_L^T and are higher than 0.5 even if Δ/δ_L^T is as large as 4.44. Therefore, even if LES is performed adopting a coarse mesh, flame surface area can be predicted reasonably well without any model of subgrid flame wrinkling by small-scale turbulence, whereas a significantly finer mesh is required to reach the same level of prediction by directly evaluating fuel consumption and heat release rates without any combustion model, i.e., by calculating the rates using the filtered fields of $\widehat{\rho}(\mathbf{x},t)$, $\widehat{T}(\mathbf{x},t)$, and $\widehat{Y}_k(\mathbf{x},t)$.

Utility of the FSD-based noCM approach to LES of premixed turbulent flames is further demonstrated in Fig. 5, which reports (a) $\delta A_F(t)$ and (b) $\delta A_T(t)$, either sampled directly from the DNS data (black dots) or computed using various normalized filter widths Δ/δ_L^T (color lines), specified in legends. Even if Δ/δ_L^T is as large as 1.33, direct integration of $|\nabla\widehat{c}_F|(\mathbf{x},t)$ or $|\nabla\widehat{c}_T|(\mathbf{x},t)$ predicts $\delta A_F(t)$ or $\delta A_T(t)$, respectively, with a reasonable accuracy of 20%–25%, cf. curves plotted in violet double-dotted-dashed lines and black dots. When Δ/δ_L^T is decreased to 0.89, the errors are further reduced by a factor of about two, see curves plotted in magenta dotted-dashed lines.

It is worth stressing that this filter width is on the order of the Taylor length scale $\lambda = 0.69\delta_L$. Therefore, the filtered quantities are associated with the inertial range of Kolmogorov turbulence, whose characteristics are controlled by the mean dissipation rate, but are weakly affected by large-scale flow peculiarities.[87] Accordingly, confinement effects, which stem from a moderate ratio (13.3 in the present case) of computational domain width to δ_L^T and are typical for contemporary DNS studies of three-dimensional complex-chemistry turbulent flames characterized by $Ka > 1$, are not expected to change the present findings regarding resolution requirements.

Moreover, results of the present *a priori* study, reported in Figs. 1–5, imply that the source term $\widehat{\rho\omega_c}(\mathbf{x},t)$ in the following well-known transport equation:[88]

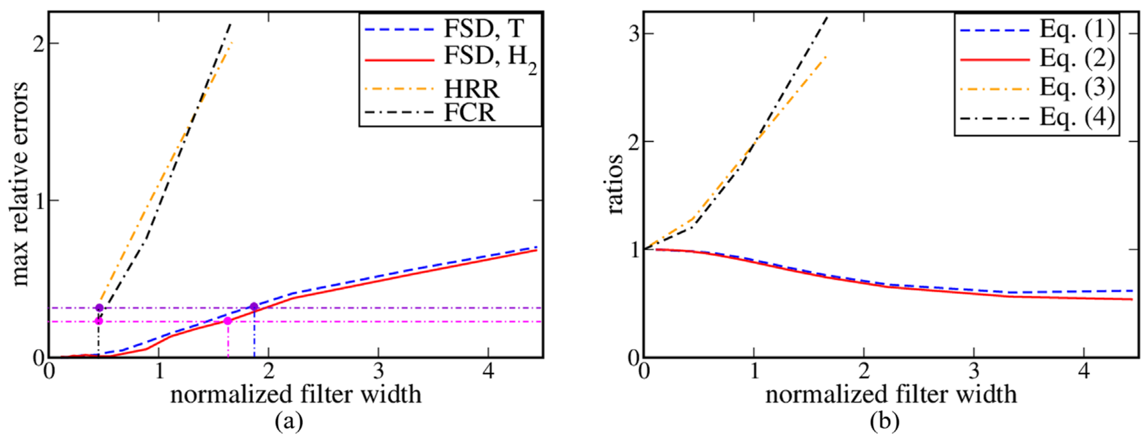

FIG. 4. (a) Maximal relative errors in evaluation of mean flame surface density (FSD), i.e., $\max\left\{\left|\overline{|\nabla c_T|}(\overline{c}) - \overline{|\nabla \widehat{c}_T|}(\overline{c})\right|\right\}\Big/\max\left\{\left|\overline{|\nabla c_T|}\right|\right\}$ or $\max\left\{\left|\overline{|\nabla c_F|}(\overline{c}) - \overline{|\nabla \widehat{c}_F|}(\overline{c})\right|\right\}\Big/\max\left\{\left|\overline{|\nabla c_F|}\right|\right\}$, heat release rate, i.e., $\max\left\{\left|\overline{\dot{\omega}_T(\rho,T,Y_k)}(\overline{c}) - \overline{\dot{\omega}_T\left(\widehat{\rho},\widehat{T},\widehat{Y}_k\right)}(\overline{c})\right|\right\}\Big/\max\left\{\overline{\dot{\omega}_T(\rho,T,Y_k)}\right\}$, and fuel consumption rate, i.e., $\max\left\{\left|\overline{\dot{\omega}_F(\rho,T,Y_k)}(\overline{c}) - \overline{\dot{\omega}_F\left(\widehat{\rho},\widehat{T},\widehat{Y}_k\right)}(\overline{c})\right|\right\}\Big/\max\left\{\left|\overline{\dot{\omega}_F(\rho,T,Y_k)}\right|\right\}$, yielded by DNS and filtered fields. (b) Ratio of time-averaged $\overline{U_t}$(orange dotted-dashed and black dotted-double-dashed lines) or time-averaged $\overline{\delta A}$ (red solid and blue dashed lines) obtained from the filtered fields $\overline{\dot{\omega}_T\left(\widehat{\rho},\widehat{T},\widehat{Y}_k\right)}$ and $\overline{\dot{\omega}_F\left(\widehat{\rho},\widehat{T},\widehat{Y}_k\right)}$ or $\overline{|\nabla \widehat{c}_T|}$ and $\overline{|\nabla \widehat{c}_F|}$, respectively, to the counterpart quantity, $\overline{U_t}$ or $\overline{\delta A}$, respectively, computed using $\overline{\dot{\omega}_T(\rho,T,Y_k)}$ and $\overline{\dot{\omega}_F(\rho,T,Y_k)}$ or $\overline{|\nabla c_T|}$ and $\overline{|\nabla c_F|}$, respectively, sampled directly from DNS data.

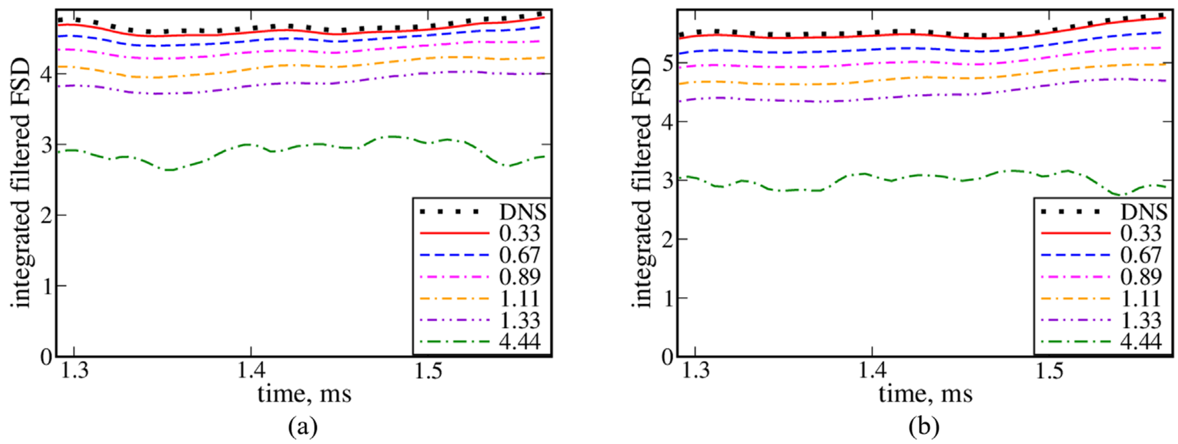

FIG. 5. Evolution of the axial integrals $\delta A(t)$, see Eqs. (1) and (2), of (a) fuel-based and (b) temperature-based flame surface density filtered using various boxes whose normalized widths Δ/δ_L^T are reported in legends.

$$\frac{\partial}{\partial t}(\hat{\rho}\tilde{c}) + \nabla\cdot(\hat{\rho}\tilde{\mathbf{u}}\tilde{c}) = \nabla\cdot(\hat{\rho}\tilde{\mathbf{u}}\tilde{c} - \widehat{\rho\mathbf{u}c}) + \widehat{\rho\omega_c} \tag{5}$$

for the Favre-filtered combustion progress variable $\tilde{c}(\mathbf{x}, t) \equiv \widehat{\rho c}/\hat{\rho}$ can simply be evaluated as follows: $\widehat{\rho\omega_c} = \rho_u S_L|\nabla\tilde{c}|$, i.e., without any model of subgrid-scale effects, because $\nabla\tilde{c}$ is directly computed using solution to Eq. (5). Note that this simplification performs better (worse) for the temperature-based (fuel-based) combustion progress variable under conditions of the present study. Such a noCM approach is expected to work reasonably well in equidiffusive mixtures provided that (i) filter width is comparable to thermal laminar flame thickness or smaller and (ii) local combustion quenching by intense turbulence does not play a statistically important role (low or moderately high Karlovitz numbers).

Nevertheless, the considered approach does not resolve all issues, because subgrid turbulent transport[88] still requires modeling, see the first term on the right-hand side of Eq. (5), as well as thermal expansion effects reviewed elsewhere.[75,89–91] Therefore, while the presented results support the discussed noCM approach for evaluating filtered flame surface area, they call also for *a posteriori* LES studies. It is worth stressing that the present work is solely restricted to flame surface density and turbulent burning velocity, whereas the subgrid turbulent transport term, which can also play an important role in premixed flames, is beyond the scope of this study. The reader interested in recent progress in modeling that term is referred to a review article by Chakraborty.[91]

It is also worth noting that, while Figs. 3–5 report results obtained by directly filtering $c(\mathbf{x}, t)$-fields, analyses of the counterpart Favre-filtered fields $\tilde{c}(\mathbf{x}, t)$ yield similar results, e.g., see Fig. 6, which shows flame-surface areas computed by substituting $\hat{c}_T(\mathbf{x}, t)$ and $\hat{c}_F(\mathbf{x}, t)$ in Eqs. (1) and (2), respectively, with the Favre-filtered $\tilde{c}_T(\mathbf{x}, t)$ and $\tilde{c}_F(\mathbf{x}, t)$, respectively. The DNS data plotted in black dotted lines are the same in Figs. 5 and 6.

Furthermore, reasonable performance of the noCM LES approach at $\Delta/\delta_L^T \approx 1$, shown in Figs. 3–5, does not result from weak fluctuations of $|\nabla c_F|(\mathbf{x}, t)$ or $|\nabla c_T|(\mathbf{x}, t)$ simulated by Dave *et al.*[59] and Dave and Chaudhuri[60] On the contrary, under conditions of that

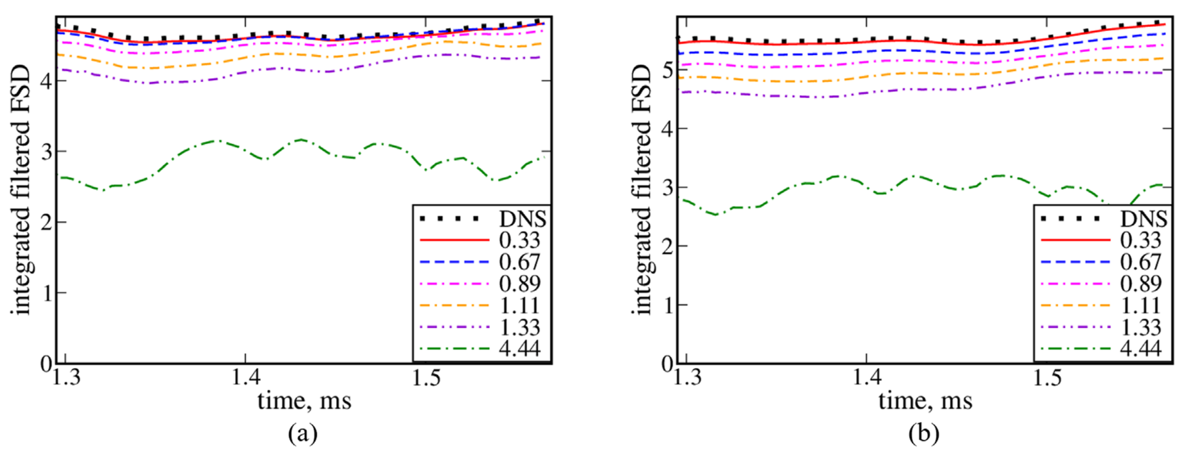

FIG. 6. Evolution of the axial integrals $\delta A(t)$, see Eqs. (1) and (2), of (a) fuel-based and (b) temperature-based flame surface density Favre-filtered using various boxes whose normalized widths Δ/δ_L^T are reported in legends.

DNS study, such fluctuations are significant. For instance, Fig. 7 shows probability density functions (PDFs) for normalized flame surface density $\delta_L^T|\nabla c_F|$ (violet dotted, black solid, and magenta dashed lines) and $\delta_L^T|\nabla c_T|$ (dotted-dashed lines) conditioned to the local values of $0.015 < c(\mathbf{x}, t) < 0.25$ (violet dotted and blue double-dotted-dashed lines), $0.045 < c(\mathbf{x}, t) < 0.55$ (black solid and brown dotted-dashed lines) and $0.075 < c(\mathbf{x}, t) < 0.85$ (magenta dashed and red dotted-dashed lines). These PDFs are wide, thus indicating significant fluctuations of $|\nabla c|(\mathbf{x}, t)$. Moreover, the PDFs peak at $\delta_L^T|\nabla c_T| \cong 1.2$ if $0.015 < c_T(\mathbf{x}, t) < 0.25$ or even $\delta_L^T|\nabla c_F| > 1.3$ if $0.015 < c_F(\mathbf{x}, t) < 0.25$. Such significant perturbations in the fields $|\nabla c|(\mathbf{x}, t)$ are associated with the influence of moderately large (when compared to δ_L^T) turbulent eddies, which strain the local inherently laminar flame. On the contrary, the documented capabilities of noCM LES approach for reasonably evaluating flame surface density filtered with $\Delta \approx \delta_L^T$ is attributed to weak influence of small-scale (when compared to δ_L^T) eddies on the local flame structure.[54]

Finally, different resolution requirements to directly evaluating filtered reaction rates $\widehat{\dot\omega}$ and filtered flame surface density $\widehat{|\nabla c|}$ are associated with different challenges to be addressed in these two cases. First, small-scale phenomena affect both $\widehat{\dot\omega}$ and $\widehat{|\nabla c|}$ and should be resolved in both cases. However, experimental and numerical results[49–58] overviewed briefly in Sec. I imply that such phenomena could be properly resolved if $\Delta \approx \delta_L$.

Second, filtering reaction rates involve an extra challenge resulting from highly non-linear dependencies of $\dot\omega_F$ and $\dot\omega_T$ on temperature.[88] Indeed, let us consider the simplest problem of a planar one-dimensional laminar flame propagating in quiescent mixture. Application of a box filter to such a flame yields the following well-known, purely numerical phenomenon, which does not result from any physical process. Figure 8 compares a spatial profile of the normalized fuel consumption rate $\dot\omega_F(x)/\max\{\dot\omega_F(x)\}$ obtained from the laminar flame (black solid line) associated with the DNS by Dave *et al.*[59] and Dave and Chaudhuri[60] with the normalized rate

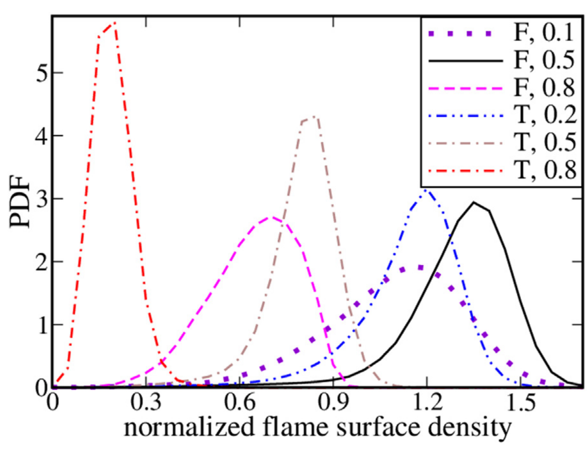

FIG. 7. Probability density functions for normalized flame surface density $\delta_L^T|\nabla c_F|$ (violet dotted, black solid, and magenta dashed lines) and $\delta_L^T|\nabla c_T|$ (dotted-dashed lines) conditioned to the local values of $c_F(\mathbf{x}, t)$ and $c_T(\mathbf{x}, t)$, respectively, specified in legends. The PDFs are sampled from the entire computational domain at 55 instants.

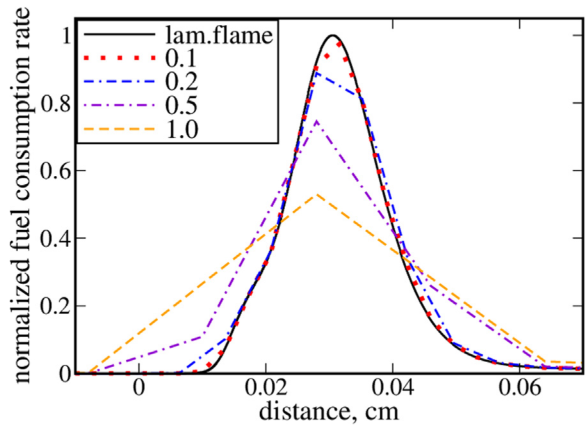

FIG. 8. Normalized fuel consumption rates $\dot\omega_F(x)/\max\{\dot\omega_F(x)\}$ sampled directly from a laminar flame (black solid line) or computed using density, temperature, and species mass fractions obtained by filtering spatial profiles of these quantities in the same laminar flame. Normalized widths Δ/δ_L^T of used box filters are reported in legends.

$\widehat{\dot\omega}_F(x)/\max\{\dot\omega_F(x)\}$ calculated using $\hat\rho$, $\hat T$, and $\hat Y_k$ computed by applying different filters to the aforementioned laminar flame. If $\Delta/\delta_L^T = 0.1$, differences between $\dot\omega_F(x)$ and $\widehat{\dot\omega}_F(x)$ are small (red dots), but such differences become notable at $\Delta/\delta_L^T = 0.2$ (blue dotted-double-dashed line), significant at $\Delta/\delta_L^T = 0.5$ (violet dotted-dashed line), and large at $\Delta/\delta_L^T = 1.0$ (yellow dashed line). This simple example clearly shows that errors yielded by noCM LES of a premixed turbulent flame can be of purely mathematical nature (averaging of a highly non-linear function over insufficiently small volume), rather than be controlled by any physical mechanism. In addition, the above simple reasoning clarifies apparent inconsistency between (i) experimental and numerical data[49–52,56–58] that indicate weak influence of small-scale (when compared to δ_L^T) eddies on premixed flames and (ii) numerical results[27–38] that show stringent resolution requirements (Δ is significantly smaller than δ_L^T) for directly evaluating fuel consumption and heat release rates.

IV. CONCLUSIONS

The present analysis of DNS data obtained earlier by Dave *et al.*[59] and Dave and Chaudhuri[60] from a moderately lean ($\Phi = 0.81$) H_2/air flame under conditions of sufficiently intense small-scale turbulence ($Ka > 1$ and a ratio of laminar flame thickness to Kolmogorov length scale is about 20) shows that the mean flame surface density and area can be predicted with acceptable accuracy (i) using a sufficiently wide filter, e.g., $\Delta/\delta_L^T = 4/3$, and (ii) spatially integrating the generalized flame surface density $|\nabla \widehat{c_F}|(\mathbf{x}, t)$ or $|\nabla \widehat{c_T}|(\mathbf{x}, t)$, evaluated directly by processing the filtered scalar field $\widehat{c_F}(\mathbf{x}, t)$ or $\widehat{c_T}(\mathbf{x}, t)$, respectively. Such an approach does not require a model of the influence of subgrid turbulent eddies on flame surface density even if LES mesh is moderately coarse (Δ is on the order of thermal laminar flame thickness). On the contrary, when calculating fuel consumption or heat release rate using filtered density, temperature, and species mass fractions, a significantly finer (by a factor of about three) mesh is required to reach a comparable prediction level. This better performance of the flame-surface-density-based noCM approach when compared to the reaction-rate-based noCM approach is associated with (i) inability of small-scale turbulent eddies to substantially wrinkle flame surface and (ii) highly non-linear dependence of fuel consumption or heat release rate on the temperature.

Nevertheless, the former noCM approach does not resolve all issues associated with modeling flame-turbulence interaction within LES framework. For instance, the problem of evaluating unresolved turbulent scaler flux was beyond the scope of the present study. Moreover, while the analyzed DNS data were obtained from a lean hydrogen-air mixture characterized by a low Lewis number, differential diffusion effects are weakly pronounced at $\Phi = 0.81$, set in the DNS. At significantly smaller equivalence ratios, e.g., $\Phi \leq 0.5$, the flame-surface-density-based noCM approach is unlikely to be sufficient, because, at least, a significant increase[48] in the mean local consumption velocity (when compared to S_L) due to differential diffusion effects should also be addressed. On the contrary, in the equidiffisive case, the approach is unlikely to be sufficient at $Ka \gg 1$, because the mean local consumption velocity is expected to be substantially reduced (when compared to S_L) due to straining of local flames by turbulent eddies.[92,93]

ACKNOWLEDGMENTS

The financial support by the Swedish Research Council (Grant No. 2023-04407) and Chalmers Area of Advance "Transport" (Grant No. C 2021-0040) is gratefully acknowledged. The author is very grateful to Professor S. Chaudhuri and Dr. H. Dave for sharing their DNS data.

AUTHOR DECLARATIONS

Conflict of Interest

The author has no conflicts to disclose.

Author Contributions

Andrei N. Lipatnikov: Conceptualization (equal); Formal analysis (equal); Funding acquisition (equal); Investigation (equal); Methodology (equal); Writing – original draft (equal); Writing – review & editing (equal).

DATA AVAILABILITY

The data that support the findings of this study are available from the corresponding author upon reasonable request.

REFERENCES

[1] D. Veynante and L. Vervisch, "Turbulent combustion modeling," Prog. Energy Combust. Sci. **28**, 193 (2002).

[2] A. N. Lipatnikov and J. Chomiak, "Turbulent flame speed and thickness: Phenomenology, evaluation, and application in multi-dimensional simulations," Prog. Energy Combust. Sci. **28**, 1 (2002).

[3] J. Janicka and A. Sadiki, "Large eddy simulation of turbulent combustion systems," Proc. Combust. Inst. **30**, 537 (2005).

[4] H. Pitsch, "Large-eddy simulation of turbulent combustion," Annu. Rev. Fluid Mech. **38**, 453 (2006).

[5] C. J. Rutland, "Large-eddy simulations for internal combustion engines—A review," Int. J. Engine Res. **12**, 421 (2011).

[6] L. Y. M. Gicquel, G. Staffelbach, and T. Poinsot, "Large eddy simulations of gaseous flames in gas turbine combustion chambers," Prog. Energy Combust. Sci. **38**, 782 (2012).

[7] E. Hawkes and S. R. Cant, "A flame surface density approach to large-eddy simulation of premixed turbulent combustion," Proc. Combust. Inst. **28**, 51 (2000).

[8] C. Fureby, "A fractal flame-wrinkling large eddy simulation model for premixed turbulent combustion," Proc. Combust. Inst. **30**, 593 (2005).

[9] Z. M. Nikolaou and N. Swaminathan, "Assessment of FSD and SDR closures for turbulent flames of alternative fuels," Flow. Turbul. Combust. **101**, 759 (2018).

[10] A. N. Lipatnikov, S. Nishiki, and T. Hasegawa, "A DNS assessment of linear relations between filtered reaction rate, flame surface density, and scalar dissipation rate in a weakly turbulent premixed flame," Combust. Theory Modell. **23**, 245 (2019).

[11] T. Dunstan, Y. Minamoto, N. Swaminathan, and N. Chakraborty, "Scalar dissipation rate modelling for large eddy simulation of turbulent premixed flames," Proc. Combust. Inst. **34**, 1193 (2013).

[12] S. Nambully, P. Domingo, V. Moureau, and L. Vervisch, "A filtered-laminar-flame PDF subgrid scale closure for LES of premixed turbulent flames. II. Application to a stratified bluff-body burner," Combust. Flame **161**, 1775 (2014).

[13] A. Donini, R. J. M. Bastiaans, J. A. van Oijen, and L. P. H. de Goey, "A 5-d implementation of FGM for the large eddy simulation of stratified swirled flame with heat loss in a gas turbine combustor," Flow. Turbul. Combust. **98**, 887 (2017).

[14] T. Brauner, W. P. Jones, and A. J. Marquis, "LES of the Cambridge stratified swirl burner using a sub-grid PDF approach," Flow. Turbul. Combust. **96**, 965 (2016).

[15] R. R. Tirunagari and S. B. Pope, "LES/PDF for premixed combustion in the DNS limit," Combust. Theory Modell. **20**, 834 (2016).

[16] A. Y. Klimenko and R. W. Bilger, "Conditional moment closure of turbulent combustion," Prog. Energy Combust. Sci. **25**, 595 (1999).

[17] S. Navarro-Martinez and A. Kronenburg, "LES-CMC simulations of a turbulent bluff-body flame," Proc. Combust. Inst. **31**, 1721 (2007).

[18] D. Farrace, K. Chung, M. Bolla, Y. Wright, K. Boulouchos, and E. Mastorakos, "A LES-CMC formulation for premixed flames including differential diffusion," Combust. Theory Modell. **22**, 411 (2018).

[19] A. Y. Klimenko and S. B. Pope, "The modeling of turbulent reactive flows based on multiple mapping conditioning," Phys. Fluids **15**, 1907 (2003).

[20] N. Iaroslavtceva, A. Kronenburg, and J. W. Gärtner, "A consistent MMC-LES approach for turbulent premixed flames," Proc. Combust. Inst. **40**, 105226 (2024).

[21] Y. Shoraka, S. Galindo-Lopez, M. J. Cleary, A. R. Masri, and A. Y. Klimenko, "Modelling a turbulent premixed flame series using an MMC-LES model with a flow-adapted flame wrinkling closure," Proc. Combust. Inst. **40**, 105296 (2024).

[22] O. Colin, F. Ducros, D. Veynante, and T. Poinsot, "A thickened flame model for large eddy simulations of turbulent premixed combustion," Phys. Fluids **12**, 1843 (2000).

[23] F. Proch and A. M. Kempf, "Numerical analysis of the Cambridge stratified flame series using artificial thickened flame LES with tabulated premixed flame chemistry," Combust. Flame **161**, 2627 (2014).

[24] H. G. Im, T. S. Lund, and J. H. Ferziger, "Large eddy simulation of turbulent front propagation with dynamic subgrid models," Phys. Fluids **9**, 3826 (1997).

[25] F. Charlette, C. Meneveau, and D. Veynante, "A power-law flame wrinkling model for LES of premixed turbulent combustion. Part II: Dynamic formulation," Combust. Flame **131**, 181 (2002).

[26] I. Yoshikawa, Y.-S. Shim, Y. Nada, M. Tanahashi, and T. Miyauchi, "A dynamic SGS combustion model based on fractal characteristics of turbulent premixed flames," Proc. Combust. Inst. **34**, 1373 (2013).

[27] F. F. Grinstein and K. Kailasanath, "Three dimensional numerical simulations of unsteady reactive square jets," Combust. Flame **101**, 192 (1995).

[28] C. Fureby, "Comparison of flamelet and finite rate chemistry LES for premixed turbulent combustion," in AIAA Paper 2007–1413 (2007).

[29] C. Duwig, K. J. Nogenmyr, C. K. Chan, and M. J. Dunn, "Large Eddy Simulations of a piloted lean premix jet flame using finite-rate chemistry," Combust Theory Modell. **15**, 537 (2011).

[30] C. Duwig, S. Ducruix, and D. Veynante, "Studying the stabilization dynamics of swirling partially premixed flames by proper orthogonal decomposition," J. Eng. Gas Turbines Power **134**, 101501 (2012).

[31] C. Duwig and M. J. Dunn, "Large eddy simulation of a premixed jet flame stabilized by a vitiated co-flow: Evaluation of auto-ignition tabulated chemistry," Combust. Flame **160**, 2879 (2013).

[32]O. Krüger, S. Terhaar, C. O. Paschereit, and C. Duwig, "Large eddy simulations of hydrogen oxidation at ultra-wet conditions in a model gas turbine combustor applying detailed chemistry," J. Eng. Gas Turbines Power **135**, 021501 (2013).
[33]C. Duwig and P. Ludiciani, "Large eddy simulation of turbulent combustion in a stagnation point reverse flow combustor using detailed chemistry," Fuel **123**, 256 (2014).
[34]B. Fiorina, R. Mercier, G. Kuenne, A. Ketelheun, A. Avdić, J. Janicka, D. Geyer, A. Dreizler, E. Alenius, C. Duwig, P. Trisjono, K. Kleinheinz, S. Kang, H. Pitsch, F. Proch, F. Cavallo Marincola, and A. Kempf, "Challenging modeling strategies for LES of non-adiabatic turbulent stratified combustion," Combust. Flame **162**, 4264 (2015).
[35]R. Ranjan, B. Muralidharan, Y. Nagaoka, and S. Menon, "Subgrid-scale modeling of reaction-diffusion and scalar transport in turbulent premixed flames," Combust. Sci. Technol. **188**, 1496 (2016).
[36]F. Nicolás-Pérez, F. J. S. Velasco, R. A. Otón-Martínez, J. R. García-Cascales, A. Bentaib, and N. Chaumeix, "Capabilities and limitations of large eddy simulation with perfectly stirred reactor assumption for engineering applications of unsteady, hydrogen combustion sequences," Eng. Appl. Comput. Fluid Mech. **15**, 1452 (2021).
[37]A. Datta, J. Mathew, and S. Hemchandra, "The explicit filtering method for large eddy simulations of a turbulent premixed flame," Combust. Flame **237**, 111862 (2022).
[38]L. Xu, Q. Fan, X. Liu, X. Cai, A. A. Subash, C. Brackmann, Z. Li, M. Aldén, and X.-S. Bai, "Flame/turbulence interaction in ammonia/air premixed flames at high Karlovitz numbers," Proc. Combust. Inst. **39**, 2289 (2023).
[39]A. Aspden, N. Zettervall, and C. Fureby, "An a priori analysis of a DNS database of turbulent lean premixed methane flames for LES with finite-rate chemistry," Proc. Combust. Inst. **37**, 2601 (2019).
[40]Y. G. Shah, J. G. Brasseur, and Y. Xuan, "Assessment of disparities in estimating filtered chemical reaction rates in LES using DNS of turbulent premixed flames," Combust. Theory Modell. **24**, 1179 (2020).
[41]H. Liu, Z. Yin, W. Xie, B. Zhang, J. Le, and H. Liu, "Numerical and analytical assessment of finite rate chemistry models for LES of turbulent premixed flames," Flow. Turbul. Combust. **109**, 435 (2022).
[42]A. N. Lipatnikov, "A priori test of perfectly stirred reactor approach to evaluating mean fuel consumption and heat release rates in highly turbulent premixed flames," Int. J. Engine Res. **24**, 4034 (2023).
[43]G. Damköhler, "Der einfuss der turbulenz auf die flammengeschwindigkeit in gasgemischen," Zs. Electrochemie **46**, 601 (1940).
[44]G. V. Nivarti and R. S. Cant, "Direct numerical simulation of the bending effect in turbulent premixed flames," Proc. Combust. Inst. **36**, 1903 (2017).
[45]W. Song, F. E. Hernández Pérez, E.-A. Tingas, and H. G. Im, "Statistics of local and global flame speed and structure for highly turbulent H_2/air premixed flames," Combust. Flame **232**, 111523 (2021).
[46]H. C. Lee, P. Dai, M. Wan, and A. N. Lipatnikov, "Displacement speed, flame surface density, and burning rate in highly turbulent premixed flames characterized by low Lewis numbers," J. Fluid Mech. **961**, A21 (2023).
[47]S. Chaudhuri and B. Savard, "Turbulent flame speed based on the mass flow rate: Theory and DNS," Combust. Flame **252**, 112735 (2023).
[48]A. N. Lipatnikov and J. Chomiak, "Molecular transport effects on turbulent flame propagation and structure," Prog. Energy Combust. Sci. **31**(1), 1 (2005).
[49]P.-H. Renard, D. Thévenin, J. C. Rolon, and S. Candel, "Dynamics of flame/vortex interactions," Prog. Energy Combust. Sci. **26**, 225 (2000).
[50]S. Kadowaki and T. Hasegawa, "Numerical simulation of dynamics of premixed flames: Flame instability and vortex-flame interaction," Prog. Energy Combust. Sci. **31**, 193 (2005).
[51]P. L. K. Paes, Y. G. Shah, J. G. Brasseura, and Y. Xuan, "A scaling analysis for the evolution of small-scale turbulence eddies across premixed flames with implications on distributed combustion," Combust. Theory Modell. **24**, 307 (2020).
[52]S. Luna and F. N. Egolfopoulos, "Local effects in vortex-flame interactions: Implications for turbulent premixed flame scaling and observables," Combust. Flame **245**, 112293 (2022).
[53]A. N. Lipatnikov, J. Chomiak, V. A. Sabelnikov, S. Nishiki, and T. Hasegawa, "A DNS study of the physical mechanisms associated with density ratio influence on turbulent burning velocity in premixed flames," Combust. Theory Modell. **22**, 131 (2018).
[54]A. N. Lipatnikov and V. A. Sabelnikov, "Influence of small-scale turbulence on internal flamelet structure," Phys. Fluids **35**, 055128 (2023).
[55]A. N. Lipatnikov, *Fundamentals of Premixed Turbulent Combustion* (CRC Press, Boca Raton, FL, 2012).
[56]A. Y. Poludnenko and E. S. Oran, "The interaction of high-speed turbulence with flames: Global properties and internal flame structure," Combust. Flame **157**, 995 (2010).
[57]N. A. K. Doan, N. Swaminathan, and N. Chakraborty, "Multiscale analysis of turbulence-flame interaction in premixed flames," Proc. Combust. Inst. **36**, 1929 (2017).
[58]U. Ahmed, N. A. K. Doan, J. Lai, M. Klein, and N. Chakraborty, "Multiscale analysis of head-on quenching premixed turbulent flames," Phys. Fluids **30**, 105102 (2018).
[59]H. L. Dave, A. Mohan, and S. Chaudhuri, "Genesis and evolution of premixed flames in turbulence," Combust. Flame **196**, 386 (2018).
[60]H. L. Dave and S. Chaudhuri, "Evolution of local flame displacement speeds in turbulence," J. Fluid Mech. **884**, A46 (2020).
[61]A. N. Lipatnikov and V. A. Sabelnikov, "An extended flamelet-based presumed probability density function for predicting mean concentrations of various species in premixed turbulent flames," Int. J. Hydrogen Energy **45**, 31162 (2020).
[62]A. N. Lipatnikov and V. A. Sabelnikov, "Evaluation of mean species mass fractions in premixed turbulent flames: A DNS study," Proc. Combust. Inst. **38**, 6413 (2021).
[63]V. A. Sabelnikov, A. N. Lipatnikov, S. Nishiki, H. L. Dave, F. E. Hernández-Pérez, W. Song, and H. G. Im, "Dissipation and dilatation rates in premixed turbulent flames," Phys. Fluids **33**, 035112 (2021).
[64]A. N. Lipatnikov and V. A. Sabelnikov, "Flame folding and conditioned concentration profiles in moderately intense turbulence," Phys. Fluids **34**, 065119 (2022).
[65]A. N. Lipatnikov, V. A. Sabelnikov, and N. V. Nikitin, "Opposite effects of flame-generated potential and solenoidal velocity fluctuations on flame surface area in moderately intense turbulence," Proc. Combust. Inst. **40**, 105238 (2024).
[66]N. Babkovskaia, N. E. L. Haugen, and A. Brandenburg, "A high-order public domain code for direct numerical simulations of turbulent combustion," J. Comput. Phys. **230**(1), 1 (2011).
[67]J. Li, Z. Zhao, A. Kazakov, and F. L. Dryer, "An updated comprehensive kinetic model of hydrogen combustion," Int. J. Chem. Kinetics **36**, 566 (2004).
[68]T. J. Poinsot and S. K. Lele, "Boundary conditions for direct simulations of compressible viscous flows," J. Comput. Phys. **101**, 104 (1992).
[69]A. N. Lipatnikov and V. A. Sabelnikov, "Karlovitz numbers and premixed turbulent combustion regimes for complex-chemistry flames," Energies **15**, 5840 (2022).
[70]F. A. Williams, *Combustion Theory*, 2nd ed. (Benjamin/Cummings, Menlo Park, CA, 1985).
[71]R. Borghi, "Turbulent combustion modeling," Prog. Energy Combust. Sci. **14**, 245 (1988).
[72]N. Peters, *Turbulent Combustion* (Cambridge University Press, Cambridge, 2000).
[73]V. A. Sabelnikov, R. Yu, and A. N. Lipatnikov, "Thin reaction zones in constant-density turbulent flows at low Damköhler numbers: Theory and simulations," Phys. Fluids **31**, 055104 (2019).
[74]J. F. Driscoll, J. H. Chen, A. W. Skiba, C. D. Carter, E. R. Hawkes, and H. Wang, "Premixed flames subjected to extreme turbulence: Some questions and recent answers," Prog. Energy Combust. Sci. **76**, 100802 (2020).
[75]A. M. Steinberg, P. E. Hamlington, and X. Zhao, "Structure and dynamics of highly turbulent premixed combustion," Prog. Energy Combust. Sci. **85**, 100900 (2021).
[76]L. Vervisch, E. Bidaux, K. N. C. Bray, and W. Kollmann, "Surface density function in premixed turbulent combustion modeling, similarities between probability density function and flame surface approaches," Phys. Fluids **7**, 2496 (1995).
[77]H. C. Lee, B. Wu, P. Dai, M. Wan, and A. N. Lipatnikov, "Area increase and stretch factor in lean hydrogen-air turbulent flames," Proc. Combust. Inst. **40**, 105687 (2024).

[78]C. E. Frouzakis, N. Fogla, A. G. Tomboulides, C. Altantzis, and M. Matalon, "Numerical study of unstable hydrogen/air flames: Shape and propagation speed," Proc. Combust. Inst. **35**, 1087 (2015).
[79]A. N. Lipatnikov, V. A. Sabelnikov, F. E. Hernández-Pérez, W. Song, and H. G. Im, "Prediction of mean radical concentrations in lean hydrogen-air turbulent flames at different Karlovitz numbers adopting a newly extended flamelet-based presumed PDF," Combust. Flame **226**, 248 (2021).
[80]H. C. Lee, A. Abdelsamie, P. Dai, M. Wan, and A. N. Lipatnikov, "Influence of equivalence ratio on turbulent burning velocity and extreme fuel consumption rate in lean hydrogen-air turbulent flames," Fuel **327**, 124969 (2022).
[81]T. L. Howarth, E. F. Hunt, and A. J. Aspden, "Thermodiffusively-unstable lean premixed hydrogen flames: Phenomenology, empirical modelling, and thermal leading points," Combust. Flame **253**, 112811 (2023).
[82]J. H. Chen and H. G. Im, "Stretch effects on the burning velocity of turbulent premixed hydrogen-air flames," Proc. Combust. Inst. **28**, 211 (2000).
[83]H. Carlsson, R. Yu, and X.-S. Bai, "Direct numerical simulation of lean premixed CH_4/air and H_2/air flames at high Karlovitz numbers," Int. J. Hydrogen Energy **39**, 20216 (2014).
[84]A. J. Aspden, M. S. Day, and J. B. Bell, "Turbulence-chemistry interaction in lean premixed hydrogen combustion," Proc. Combust. Inst. **35**, 1321 (2015).
[85]M. Rieth, A. Gruber, F. A. Williams, and J. H. Chen, "Enhanced burning rates in hydrogen-enriched turbulent premixed flames by diffusion of molecular and atomic hydrogen," Combust. Flame **239**, 111740 (2022).
[86]H. C. Lee, P. Dai, M. Wan, and A. N. Lipatnikov, "A numerical support of leading point concept," Int. J. Hydrogen Energy **47**, 23444 (2022).
[87]L. D. Landau and E. M. Lifshitz, *Fluid Mechanics* (Pergamon Press, Oxford, UK, 1987).
[88]T. Poinsot and D. Veynante, *Theoretical and Numerical Combustion*, 2nd ed. (Edwards, Philadelphia, PA, 2005).
[89]A. N. Lipatnikov and J. Chomiak, "Effects of premixed flames on turbulence and turbulent scalar transport," Prog. Energy Combust. Sci. **36**(1), 1 (2010).
[90]V. A. Sabelnikov and A. N. Lipatnikov, "Recent advances in understanding of thermal expansion effects in premixed turbulent flames," Annu. Rev. Fluid Mech. **49**, 91 (2017).
[91]N. Chakraborty, "Influence of thermal expansion on fluid dynamics of turbulent premixed combustion and its modelling implications," Flow. Turbul. Combust. **106**, 753 (2021).
[92]K. N. C. Bray and R. S. Cant, "Some applications of Kolmogorov's turbulence research in the field of combustion," Proc. Roy. Soc. London A **434**, 217 (1991).
[93]D. Bradley, A. K. C. Lau, and M. Lawes, "Flame stretch rate as a determinant of turbulent burning velocity," Phil. Trans. R Soc. Lond. A **338**, 359 (1992).